Experimental demonstration of attractor annihilation in a multistable fiber laser

A. N. Pisarchik, Yu. O. Barmenkov, and A. V. Kir'yanov
Centro de Investigaciones en Optica, Loma del Bosque 115, Lomas del Campestre, 37150 Leon, Guanajuato, Mexico
(Received 17 June 2003; published 30 December 2003)

We report on the experimental open-loop control of generalized multistability in a system with coexisting attractors. The experimental system is an erbium-doped fiber laser with pump modulation of the diode laser. We demonstrate that additional weak harmonic modulation of the diode current annihilates one or two stable limit cycles in the laser. The ability of the method to select a desired state is illustrated through a codimension-two bifurcation diagram in the parameter space of the frequency and amplitude of the control modulation. We identify main resonances on the bifurcation lines (annihilation curves) and evaluate conditions for attractor annihilation.

DOI: 10.1103/PhysRevE.68.066211 PACS number(s): 05.45.Gg, 05.45.Ac, 42.55.Lt, 42.65.Sf

I. INTRODUCTION

Many nonlinear systems exhibit the coexistence of multiple dynamic equilibrium states in some regions of parameter space. This phenomenon, referred to as generalized multistability, is found in a variety of systems from different fields, including electronics [1], optics [2], mechanics [3], and biology [4], in addition to some standard models such as Hénon map [5], Duffing, van der Pol [6], and Lorenz equations [7]. In such multiattractor systems the final state depends crucially on the initial conditions. However, in many practical situations multistability can create inconvenience, for instance, in construction of a commercial device with determinate characteristics. Below, we cite several examples of where we believe multistability may represent a problem for applications.

(i) The idea of optical communications using transmitters and receivers operating in nonlinear dynamical regimes has recently attracted the attention of many researchers. This was first studied using electronic circuits [8] and then proposed in solid-state [9], fiber [10], semiconductor [11], and microchip lasers [12]. However, the lasers can exhibit multistability under pump modulation [13,14], loss modulation [15], or optical injection [16]. Such a behavior may give rise to technological difficulties in efficient communication because the system may suddenly jump from one attractor to the other and some information may be lost. Therefore, under these circumstances multistability might be undesirable.

(ii) Solid-state lasers with nonlinear mirrors may have more than one stable steady states [17]. As a result, small fluctuations in the pump rate can provoke sudden switches between coexisting attractors that impairs the stability of the laser output. Such a behavior may restrict the development of practical devices based on these lasers for signal or data processing [18].

(iii) In solid-state laser technology, the use of the intracavity frequency doubling to transform the fundamental infrared laser radiation into visible radiation by the processes of second harmonic and sum-frequency generation is restricted due to irregular fluctuations of the output intensity. This behavior, referred to as the green problem [19] arises from a coupling of the longitudinal modes of the laser by sum-frequency generation, which occurs in the intracavity second harmonic generation crystal. Several feedback control methods [20] have been developed to stabilize unstable periodic orbits embedded in a chaotic attractor and suppress undesired fluctuations. However, the complexity and strong nonlinearity of the system result in coexistence of multiple attractors in this laser [19]. Thus, not all instabilities can be suppressed by the feedback control. We believe that an appropriate control of multistability may help in resolving the green problem.

(iv) A time-delayed feedback is known to be an efficient tool for continuous-time control of chaotic systems [21]. However, at certain conditions the delay in feedback stabilizes not only a single periodic orbit, but simultaneously several periodic orbits embedded in a chaotic attractor and by such a way it makes the system multistable [22]. This phenomenon was observed in an electro-optical bistable device [23] and in a laser diode pumped hybrid bistable system [24]. Thus, multistability imposes the restriction on the delayed feedback control to stabilize a particular periodic orbit.

(v) In future generation nuclear reactors with two-phase natural circulation loops [25], a coolant flow design is important to avoid all sorts of instabilities which may lead to a holocaust. Therefore, multiple coexisting attractors in this system might be considered as harmful while designing the operating regime of the coolant flow.

(vi) Recently much attention has been paid to the superconductivity electronic devices, Josephson junctions, which have been suggested as voltage standards, oscillators, and detectors [26]. To increase the sensitivity or power output beyond what one device would provide, the devices are coupled into array. However, complicated forms of coupling can lead to a coexistence of several stable phase configurations. In this case the coupled system is multistable: which of these configurations is realized depends on the initial conditions (in phase space this corresponds to existence of several attractors with different basins). This runs the risk of an asynchronous (out-of-phase) behavior of the system [27] and deteriorates the efficiency of the device. Other examples where the existence of the multiattractor behavior in an array of coupled oscillators may be undesirable are robotics, laser arrays, frequency dividers, physiology, etc. (see Ref. [28], and references therein).

(vii) In medical science, a cardiac arrythmia has been successfully suppressed to a normal cardiac rhythm with the use of chaos control methods, i.e., a period-1 state has been stabilized [29]. However, under certain circumstances, the coexistence of a stable period-2 rhythm is also observed [30]. It is evident that bistability in cardiac rhythm is undesirable.

Thus, the above few examples demonstrate that the control of multistability in systems with coexisting attractors becomes an important problem in applied nonlinear science.

During the last decade the active search was underway to find possibilities to control systems with coexisting attractors. Some authors demonstrated that it is possible to enhance multistability by steering trajectories toward a desired attractor by first making the system chaotic [31] or noisy [32] so that the regions associated with the original attractors are randomly visited [33], and then applying a correction signal to the variable to drive the multistable system to the preselected attractor [34], regardless of where the trajectory is initialized. These methods do not allow a complete destruction of undesired attractors, they just change the basins of attraction of attractors so that a trajectory is attracted to a desired state. However, the system may involuntary switch from this state to the other if the initial conditions suddenly change, for example, due to any instabilities.

Another approach in controlling multistability was suggested in Refs. [35,36]. The authors call up the idea of complete annihilation of undesirable attractors in order to make the system monostable. Distinct from many previous works on the control of chaos, where "control" means that it is possible to obtain some specific solutions of the system, in the context of attractor annihilation the control intends killing the undesired solutions so that only one remains. It was shown that stable fixed points or limit cycles can be annihilated by a weak periodic modulation applied to a system parameter [35,36] or by adding noise [7]. In the former case, due to the resonant interaction of the modulation frequency with the frequency of damped oscillations of the attractor, the parametrical modulation induces chaos and the attractor is destroyed in boundary crisis. Similar behavior is observed in the latter case, where a stochastic resonancelike behavior is embodied in a Hopf-bifurcationlike sequence to chaos evicted by noise, where the strength of noise acts as a bifurcation parameter [7]. The annihilation methods have been developed with different theoretical models, including the Hénon map [36–38], lasers [14,39], coupled Duffing oscillators [40], a time-delayed logistic map [39], and Lorenz equations [7]. However, in spite of their evident universality and simplicity, these methods have not been so far realized experimentally in a multistable system.

In this paper, we provide an experimental evidence for annihilation of various coexisting attractors, thus making the system monostable. Specifically, we demonstrate how multiple attractors created in a pump-modulated erbium-doped fiber laser can be selectively destroyed by adding small and weak modulation to the diode current of the pump laser and evaluate best conditions for annihilation of a particular attractor. We use the laser as a paradigm of a dynamical system, which exhibits damped oscillations inherent in many complex systems, when it is subjected to an external perturbation.

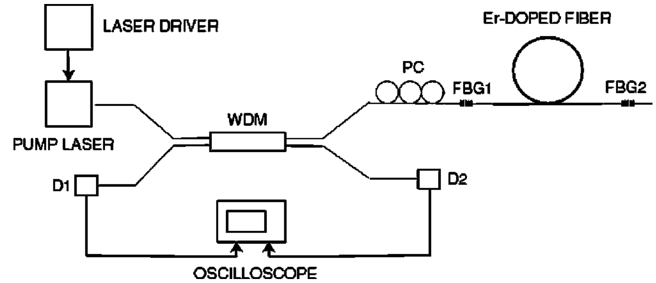

FIG. 1. Experimental setup. WDM is the wavelength-division multiplexing coupler, PC is the polarization controller, FBG1 and FBG2 are the Bragg gratings, and D1 and D2 are the photodetectors.

Apart of the great importance for technological applications [41], the erbium-doped fiber laser is a rich dynamical system with many complex features. Different dynamical regimes, bistability, and chaos have been observed in the fiber laser with modulated parameters [42]. Moreover, for a wide range of parameters the erbium-doped laser displays the coexistence of multiple periodic and chaotic attractors [15], each of which is determined by initial conditions. An important difference of the heavily erbium-doped fiber laser from other class-*B* lasers is that the former laser represents self-pulsations at the fundamental laser frequency [43], i.e., this laser acts as an autonomous system. In this sense the dynamics of the erbium-doped fiber laser under external modulation is more sophisticated than the dynamics of other class-*B* lasers because the interaction of the modulation frequency with the frequency of self-pulsations may lead to frequency locking, quasiperiodicity, and chaos [44]. However, frequency locking takes place only in the low-frequency range, where the modulation frequency is lower than the half of the fundamental laser frequency. At higher frequencies the erbium-doped fiber laser acts as other class-*B* lasers, i.e., as a nonautonomous system. In this work we consider a relatively high-frequency range where three periodic attractors coexist, and where the frequency locking has no influence on the laser dynamics.

The paper is organized as follows. In Sec. II we describe our experimental setup of the erbium-doped fiber laser and present bifurcation diagrams demonstrating coexistence of multiple attractors. We determine the parameter domain where different dynamical regimes coexist. In Sec. III we show how the coexisting attractors can be destroyed by periodic modulation of the pump current and plot annihilation curves in space of the control parameters. The mechanisms underlying the annihilation phenomenon are discussed in Sec. IV. Finally, the main conclusions are given in Section V.

II. COEXISTING ATTRACTORS

A. Experimental setup

In our experiments, the erbium-doped fibre laser is pumped by a commercial laser diode (wavelength 976 nm, maximum pump power 300 mW) through a wavelength-division multiplexing coupler (WDM) and polarization controller (PC) (Fig. 1). The laser cavity of 1.5-m length is

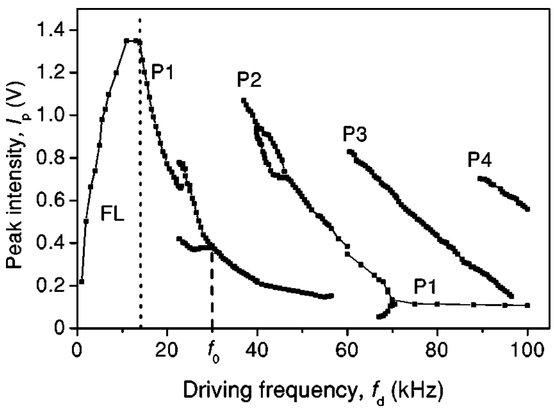

FIG. 2. Bifurcation diagrams of peak laser intensity with driving frequency as control parameter at 50% modulation depth of pump laser diode current. The fundamental laser frequency f_0 is shown by the dashed line. The dotted line bounds the frequency locking region (FL). $P1$, $P2$, $P3$, and $P4$ are the period-1, period-2, period-3, and period-4 regimes.

formed by a piece of a commercial (from IPHT Jena) heavily doped erbium fiber (Er_2O_3-concentration 2300 ppm) of 70-cm length and a core diameter of 2.7 μm, and two fiber Bragg gratings (FBG1 and FBG2) with a 2-nm FWHM (full width on half magnitude) bandwidth and reflectivity of 91% and 95% at a 1560-nm wavelength. Output power of the pumping laser diode and fiber laser are recorded with photodetectors D1 and D2 and analyzed with an oscilloscope and a Fourier spectrum analyzer. The output power of the diode laser depends linearly on the laser diode current.

Without any external modulation, the output power of the erbium-doped fiber laser represents self-oscillations at fundamental laser frequency f_0 (in our case $f_0 = 30$ kHz). Such a self-pulsing behavior may be attributed to the presence of a saturable loss due to erbium ion pairs and(or) excited state absorption in the heavily doped fiber [45,46]. The harmonic signal, $A_d \sin(2\pi f_d t)$ (where A_d and f_d are the driving amplitude and frequency), applied from a signal generator to the laser driver causes harmonic modulation of the diode current with f_d. In our experiments, the signal with $A_d = 800$ mV results in 50% modulation depth of the pump power, while the average diode current is fixed at 40 mA.

B. Bifurcation diagrams

The dynamics of the parametrically modulated erbium-doped fiber laser was studied extensively by various authors [44] who demonstrated the coexistence of multiple attractors at certain laser parameters. The bifurcation diagram of peak intensity I_p of the fiber laser with f_d as a control parameter for $A_d = 800$ mV is shown in Fig. 2. This diagram is obtained by a slow increase and decrease of the control parameter. The laser dynamics is ruled mainly by the ratio of f_d to fundamental laser frequency f_0 defined by the saturable loss in the fiber and pump power. In our experiments $f_0 = 30$ kHz for the pump power of 15 mW. In the low-frequency range ($f_d < 14$ kHz), we observe frequency locking, quasiperiodicity, and chaos. The laser dynamics in this region (FL) represents a well known structure such as Arnold

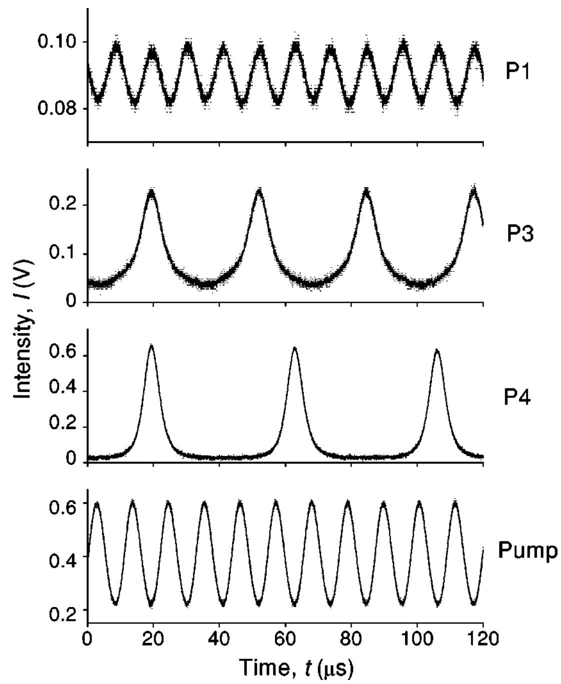

FIG. 3. Time series demonstrating coexistence of different dynamical regimes at $f_d = 93$ kHz and $A_d = 0.8$ V. The lower trace shows the pump modulation signal.

tongues. With increasing f_d, different attractors appear in saddle-node and period-doubling bifurcations giving rise to generalized multistability. In this paper we are interested in the frequency range where three periodic attractors coexist. As seen from Fig. 2 this occurs at the driving frequencies $f_d > 90$ kHz.

When we fix the driving frequency at $f_d = 93$ kHz, three periodic attractors coexist within certain region of the driving amplitudes. The time series illustrating the coexistence of the period-1, period-3, and period-4 regimes are shown in Fig. 3. In the lower trace in the same figure we show for comparison the intensity of the pump diode laser. The coexistence of three attractors is also demonstrated in Fig. 4, where we display the bifurcation diagram of the laser peak intensity with respect to A_d. For small values of the driving amplitude, $A_d < 300$ mV, only one (period-1) attractor exists, so that the laser behaves almost as a linear damped oscillator periodically oscillating with frequency f_d. As A_d is increased, the period-4 and period-3 attractors appear in the corresponding saddle-node bifurcations (SNBs). The SNB points (S_3 and S_4) are found experimentally by slow decreasing A_d until the laser switches from the period-3 or from the period-4 to the period-1 regime.

III. ATTRACTOR ANNIHILATION

In order to control the multistability, we apply the additional harmonic modulation, $A_c \sin(2\pi f_c t)$, to the pump current, so that the total signal from the generator takes the form

$$A = A_d[1 + A_c \sin(2\pi f_c t)]\sin(2\pi f_d t), \tag{1}$$

where A_c and f_c are the control amplitude and frequency.

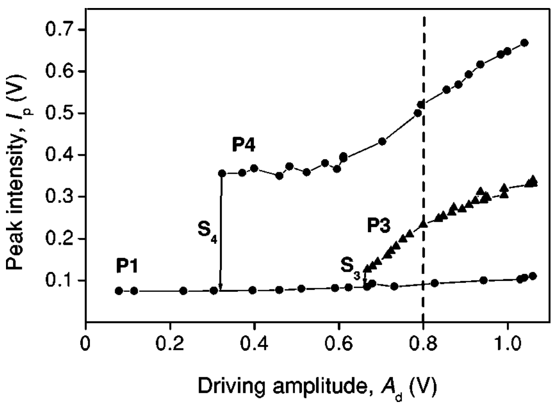

FIG. 4. Bifurcation diagrams of peak laser intensity with driving amplitude as control parameter at $f_d = 93$ kHz. The arrows show the jumps to the period-1 regime (P1) from the period 3 (P3) and the period 4 (P4), which occur in the saddle-node bifurcation points, S_3 and S_4, when A_d is decreased. The dashed line indicates the initial position of driving amplitude $A_d = 0.8$ V when the control modulation is applied.

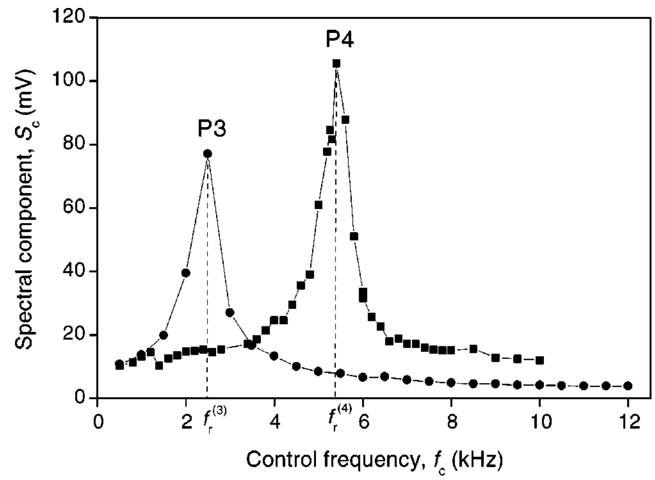

FIG. 5. Linear laser responses to control modulation with $m = 0.01$ at $f_d = 93$ kHz and $A_d = 0.8$ V. The maxima appear at resonance frequencies $f_r^{(3)}$ and $f_r^{(4)}$ of the period-3 and period-4 attractors.

The value A_d is chosen to be in the range of coexistence of the attractors, i.e., $A_d = 800$ mV (dashed line in Fig. 4). The control amplitude A_c is chosen such that the maximum value of A during the control modulation does not cross the SNB points where the period-3 and period-4 attractors are born, i.e., $A_c < 150$ mV for the period-3 attractor and $A_c < 250$ mV for the period-4 attractor.

The goal of this type of the control is to annihilate one or two of the coexisting attractors so that the final state of the system is the period-1 limit cycle. In practical situations, it is important to be able to drive most trajectories to the desirable attractor in an efficient and economic way, i.e., by using only small perturbations to an accessible parameter. However, for trajectories deep in the basin of an undesired attractor, small perturbations cannot change the attractor to which the trajectory is asymptoting. Pecora and Carroll [31] demonstrated that in periodically driven dynamical systems, multiple basins of attraction of attractors can be eliminated by replacing the periodic driving by some appropriately chosen but somewhat large-amplitude chaotic driving. In this work, instead of changing the periodic driving to chaotic one, we add the additional periodic (control) modulation to the same system parameter Eq. (1). As in the method of Pecora and Carroll, the amplitude of the control modulation is not small, so that the control is nonlinear. However, we will show that the control goal can be achieved by *relatively* small control, i.e., $A_c \ll A_d$.

When the amplitude of the control modulation is small [$m < 0.05$, where $m = (A_d - A_c)/(A_d + A_c)$ is the modulation depth], the laser response to the control modulation is almost linear and appears as a slow envelope of the laser pulses in each nonlinear regime. In other words, this is the linear response of the nonlinear system to small perturbations. The amplitude of this slow envelope depends on the control frequency and has a maximum at the resonant frequency of the attractor, $f_r^{(n)}$ (n is the attractor period). In our experiments we estimate $f_r^{(n)}$ from a Fourier transform of the generated sequence of laser pulses. In Fig. 5 we plot the f_c spectral component, S_c, in the power spectrum of the laser output versus the control frequency for the laser oscillating in the period-3 and period-4 regimes at $m = 0.01$. One can see that the resonance frequency for the period-3 attractor in $f_r^{(3)} \approx 2.5$ kHz and for the period-4 attractor is $f_r^{(4)} \approx 5.4$ kHz.

While m is increased, the laser response to the control modulation becomes nonlinear which leads to the attractor annihilation. The annihilation curves for the period-3 and period-4 attractors in the (f_c, m) parameter space are shown in Fig. 6. Each attractor exists for the control parameters below the corresponding curve, while above the upper curve the system is monostable, i.e., only the period 1 exists. While the parameters f_c and m approach the annihilation curves, the system in each of the regimes undergoes a sequence of

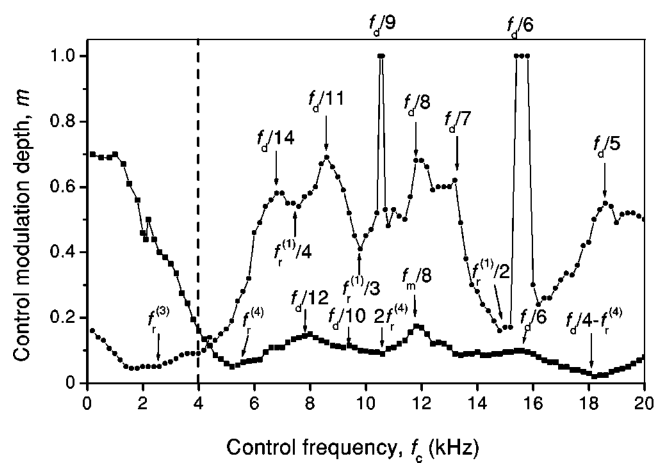

FIG. 6. Codimension-two bifurcation diagram in (f_c, m)-parameter space at $A_d = 0.8$ V and $f_d = 93$ kHz. The curves connecting the dots and squares are the crisis lines (annihilation curves) for the period-3 and period-4 attractors, respectively. Some resonances are marked with the arrows. The dashed line indicates the control frequency at which the time series in Fig. 7 are recorded.

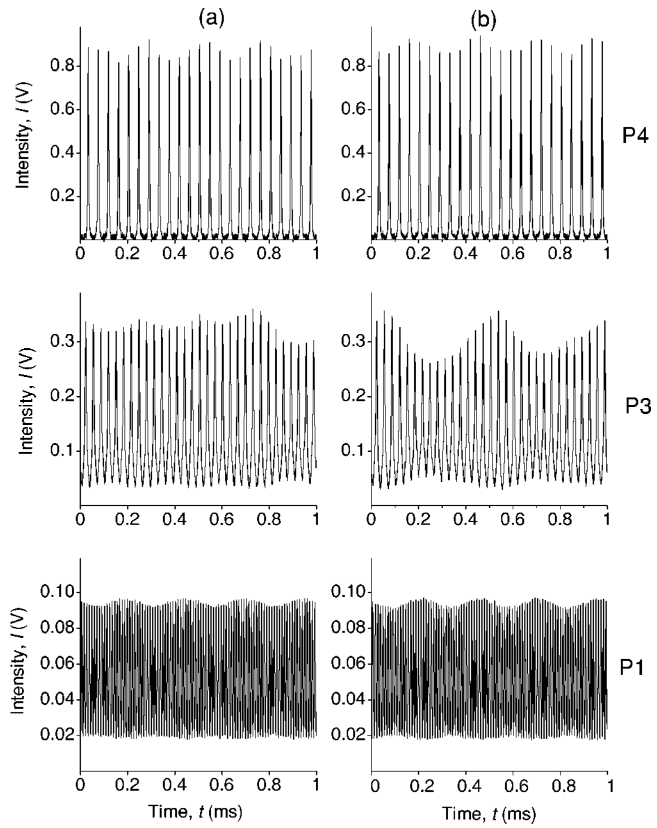

FIG. 7. Time series demonstrating effect of control modulation with $f_c = 4$ kHz on period-1, period-3, and period-4 attractors for (a) $m = 0.05$ and (b) $m = 0.06$. $f_d = 93$ kHz and $A_d = 0.8$ V. Close to the annihilation curve the laser undergoes the period-doubling bifurcation at control frequency (middle trace in (b)).

period-doubling bifurcations in control frequency [i.e., in the slow envelope, as shown in the middle trace of Fig. 7(b)] terminated by chaos and crisis of the attractor. After destruction, the chaotic transients jump to the basin of attraction of the neighboring attractor. The sequence of the period doubling and chaos are localized in a narrow parameter range close to the annihilation curves slightly below them. In fact, the annihilation curves in Fig. 6 are crisis lines. One can see that these curves have several peaks and dips. In the dips the conditions for the control is better, because the modulation amplitude required for the annihilation is smaller, whereas in the peaks larger m is required for the annihilation. Moreover, at some modulation frequencies it is impossible to kill the period-3 attractor. Now consider the origin of such a behavior of the annihilation curves.

IV. DISCUSSION

The physical mechanism underlying the annihilation phenomenon is described in Ref. [36]. The attractor annihilation results from a resonant interaction of the control frequency with the frequency of damped oscillations of the associated attractor, i.e., with the frequency at which a trajectory initiated in the basin of attraction of the corresponding attractor exhibits damped oscillations before being attracted to the limit cycle. This frequency is close to, but slightly lower than, $f_r^{(n)}$ due to the damping, as typical for a damped oscillator [47]. When the system is subjected to two-frequency modulation with incommensurate frequencies, the attractor becomes quasiperiodic with a toroidal surface in a three-dimensional phase space. Moreover, the basin of attraction of the attractor also changes [37]. The new attractor is less stable in the sense that the absolute value of the leading negative Lyapunov exponent is smaller, i.e., it is closer to zero [37]. While the control amplitude is increased, each of the tori transforms to a chaotic attractor which then undergoes boundary crisis at the certain value of f_c and the torus disappears. The boundary crisis occurs when the chaotic attractor reaches the boundary of its basin of attraction.

The appearance of the peaks and dips on the annihilation curves in Fig. 6 can be understood if we take into account the resonant interaction of three main frequencies in the system, f_d, f_c, and $f_r^{(n)}$. We identify some of the extrema in the figure, but not all of them. One can see that several dips on the annihilation curves appear when the control frequencies is close to the resonance frequencies of the attractors (Fig. 5) or their harmonics. This confirms the prediction made in Ref. [36]: the best condition for attractor annihilation is realized (i.e., the smallest control amplitude is required) when $f_c \approx f_r^{(n)}$. Actually, the minima coincide with the frequencies of damped oscillations that are slightly lower than $f_r^{(n)}$. As seen from Fig. 6, when the control is applied at these frequencies, the period-3 and period-4 attractors can be destroyed with $m = 0.05$, i.e., by only 5% control modulation of the driving amplitude. Other local minima on the annihilation curves may appear at difference frequencies of $f_r^{(n)}$ (for example, as the dip at $f_c = f_d/4 - f_r^{(4)}$ for the period-4 attractor) and at subharmonics of the fundamental laser frequency $f_r^{(1)} \equiv f_0$ (for example, when $f_c = f_r^{(1)}/2$ and $f_c = f_r^{(1)}/3$ for the period-3 attractor). The dips at the latter frequencies arise because the control at subharmonics of the fundamental laser frequency gives the preference for the period-1 attractor, and hence the other attractors can be easier destroyed. On the contrary, the control at subharmonics of the driving frequency improves the stability of the period-3 and period-4 attractors (the absolute value of the leading Lyapunov exponent increases) which makes it difficult or even impossible to destroy them. For instance, when $f_c \approx f_d/9$ or $f_c \approx f_d/6$ the period-3 attractors cannot be destroyed even at $m = 1$. Therefore, the interaction of f_c with f_d is a reason of the several maxima on the annihilation curves. However, some peaks and dips do not appear if the resonant frequency which stabilizes one of the attractors is close to another resonant frequency which destabilizes it. For example, the peak at $f_d/9$ does not appear on the annihilation curve for the period-4 attractor, because this frequency almost coincides with the second harmonic of $f_r^{(4)}$, which leads to the resonant destruction of the attractor. However, the frequency $f_r^{(4)}$ has no effect when the laser operates in the period-3 regime. Thus, the shape of the annihilation curves in the high-frequency range ($f_c > f_r^{(n)}$) is defined by the competition between the main frequencies of the system.

The important feature of this control is that the attractors can be annihilated with a relatively *slow* modulation as compared with the driving frequency and the frequency of the attractor to be controlled. The slow control is more convenient for practical applications because it can be realized with a *weak* modulation of the driving amplitude. By "weak" modulation we imply that the change in the driving amplitude, $A_d A_c$ [see Eq. (1)] in the uncontrolled case, will lead to no bifurcation of the attractors, i.e., parameter $A = A_d(1-A_c)$ is smaller than the stationary position of each SNB point (Fig. 4). In practice, the control signal can be supplied from the same signal generator as amplitude modulation of the driving signal. Moreover, the control does not require any *a priori* knowledge of the system behavior because the first dips on the annihilation curves can be easily found in experiments when f_c is slowly increased from zero. It is seen from Fig. 6 that the control modulation with $f_c < f_r^{(n)}$ also can destroy the attractors, but m should be larger. However, the modulation at very low frequencies ($f_c \to 0$) corresponds to a quasistationary change in the driving amplitude and the attractor dies in the corresponding SNB when the modulated parameter A reaches the SNB point (see Fig. 4). This occurs when $m=0.16$ for the period-3 regime and $m=0.7$ for the period-4 regime. Such a slow modulation is not interesting for the control, because the different system state can be easier achieved by just changing the driving amplitude without any additional modulation.

Another feature of the system subjected to parametrical modulation is a dynamical shift of bifurcation points. When a parameter is changed in time so that the system passes through a bifurcation point, the bifurcation delays in time and appears at a different instant value of the parameter [48]. Such a dynamical shift of the bifurcation point depends on the velocity at which the parameter is changed. Similar behavior occurs when the parameter is periodically modulated in the vicinity of the bifurcation point [37,49,50]. In the latter case the shifted position of the bifurcation point depends on the frequency and amplitude of the parameter modulation. This phenomenon was observed for different critical points, including the period-doubling bifurcation [49], SNB, and crisis point [37,50]. The annihilation curve for the period-3 attractor in Fig. 6 demonstrates the dynamical shift of the SNB point. For $f_c > 5$ kHz the period-3 attractor still exists when parameter A crosses the stationary SNB (S_1 in Fig. 2), i.e., for $m > 0.16$. As was shown in Ref. [37], the shift of critical points results from a deformation of the basins of attraction of attractors and a change in their fractal dimensions. The shift of the SNB point is not observed for the period-4 attractor, because A during the modulation never reaches the stationary position of the SNB point (S_2 in Fig. 4), i.e., $m < 0.7$. The period-4 attractor is annihilated at much smaller control amplitude because the basin of attraction of this attractor is smaller.

The important advantage of our method is that each of the coexisting attractors can be *selectively* destroyed by the control modulation with properly chosen amplitude and frequency. As seen from Fig. 6, the annihilation curves for the period-3 and period-4 attractors are crossed at $f_c = 4.3$ kHz, where two crisis lines coincide. Close to this point, it is possible to destroy selectively either the period-3 or period-4 attractor by changing just the control frequency f_c to be slightly before or after the crossing point. Moreover, by choosing m to be slightly above the crossing point it is possible to kill both attractors with smallest value of the control amplitude. Figure 7 displays with time series the laser oscillations for the control parameters slightly below the annihilation curve for the period-3 attractor. At $f_c = 4$ kHz and $m = 0.05$ the laser oscillates either in the period-1 (P1), period-3 (P3), or period-4 (P4) regimes depending on the initial conditions [Fig. 7(a)]. Closer to the annihilation curve for the period-3 attractor (at $m=0.06$), the period doubling appears in control frequency (in the slow envelope) of the laser pulses [middle trace in Fig. 7(b)] and the amplitude of the slow modulation increases [compare with Fig. 7(a)]. However, almost no changes occur in the period-4 and period-1 regimes. When m is further increased so that the control parameters cross the annihilation curve for the period-3 attractor (at $m=0.07$), the period 3 disappears. Then, closer to the annihilation curve for the period-4 attractor (at $m=0.14$) the laser undergoes the period-doubling sequence to chaos in the slow envelope of the period-4 regime. Finally, the period 4 also disappears (at $m=0.16$) and only the period 1 remains. Similar behavior is observed when we fix m and manipulate f_c in the vicinity of the annihilation curves.

V. CONCLUSIONS

In this paper we have reported on the experimental observation of attractor annihilation in a multiattractor system. With an example of the pump-modulated erbium-doped fiber laser we have demonstrated that multiple coexisting attractors can be selectively destroyed by adding a harmonic parametrical modulation with properly chosen control parameter values. We have provided the experimental evidence of the ability of the annihilation method to control multistability and flexibility in manipulating the system's dynamics to select a desired behavior or to make the system monostable. In fact, this laser is a device with a well-defined number of coexisting states. We have demonstrated that the coexisting attractors can be destroyed by slow (two orders of magnitude lower than the driving frequency and one order of magnitude lower than the frequency of the attractor to be controlled) and weak (5% of the driving amplitude) control modulation. The method does not require a permanent tracking for the system state; once the control is applied, the undesired state never appears, because it does not exist.

We have proved theoretical predictions that this effect has a resonant character and identified some resonances on the annihilation curves. The shape of the annihilation curve is defined by the resonant interaction of the control frequency with other main frequencies in the system: the driving frequency, the frequencies of the attractor and its damped oscillations, and the fundamental laser frequency. The best condition for the control (minimal amplitude of the control modulation) is realized when the control frequency is close to the frequency of damped oscillations of the attractor to be annihilated. We believe that the results of this paper will be useful for experimentalists in many areas of science, who work with multiattractor systems and wish to avoid undesired attractors or to make the system monostable.

ACKNOWLEDGMENTS

This work was supported by the University of California Institute for Mexico and the United States (UC MEXUS) and Consejo Nacional de Ciencia y Tecnologia (CONACyT).

[1] J. Maurer and A. Libchaber, J. Phys. (Paris), Lett. **41**, 515 (1980).

[2] E. Brun, B. Derighetti, D. Meier, R. Holzner, and M. Raveni, J. Opt. Soc. Am. B **2**, 156 (1985); J.R. Tredicce, F.T. Arecchi, G.P. Puccioni, A. Poggi, and W. Gadomski, Phys. Rev. A **34**, 2073 (1986); D. Dangoisse, P. Glorieux, and D. Hennequin, *ibid.* **36**, 4775 (1987); H.G. Solari, E. Eschenazi, R. Gilmore, and J.R. Tredicce, Opt. Commun. **64**, 49 (1987).

[3] J. M. T. Thompson and H. B. Stewart, *Nonlinear Dynamics and Chaos* (Wiley, Chichester, 1986).

[4] J. Foss, A. Longtin, B. Mensour, and J. Milton, Phys. Rev. Lett. **76**, 708 (1996); E. Simonotto, M. Riani, C. Seife, M. Roberts, J. Twitty, and F. Moss, *ibid.* **78**, 1186 (1997); P. Cordo, J.T. Inglis, S. Verschueren, J.J. Collins, D.M. Merfeld, S. Rosenblum, S. Buckley, and F. Moss, Nature (London) **383**, 769 (1996).

[5] J. Curry, Commun. Math. Phys. **68**, 129 (1979).

[6] J. Guckenheimer and P. Holmes, *Nonlinear Oscillations, Dynamical Systems, and Bifurcation of Vector Fields* (Springer-Verlag, New York, 1983).

[7] J.B. Gao, Wen-wen Tung, and Nageswara Rao, Phys. Rev. Lett. **89**, 254101 (2002).

[8] K.M. Cuomo and A.V. Oppenheim, Phys. Rev. Lett. **71**, 65 (1993).

[9] P. Colet and R. Roy, Opt. Lett. **19**, 2056 (1994).

[10] G.D. Van Wiggeren and R. Roy, Science **279**, 1198 (1998).

[11] C.R. Mirasso, P. Colet, and P. García-Fernández, Phot. Tech. Lett. **8**, 299 (1996).

[12] A. Uchida, M. Shinozuka, T. Ogawa, and F. Kannari, Opt. Lett. **24**, 890 (1999).

[13] W. Lauterborn and R. Steinhoff, J. Opt. Soc. Am. B **5**, 1097 (1988).

[14] A.N. Pisarchik and B.F. Kuntsevich, IEEE J. Quantum Electron. **38**, 1594 (2002).

[15] J.M. Saucedo-Solorio, A.N. Pisarchik, A.V. Kir'yanov, and V. Aboites, J. Opt. Soc. Am. B **20**, 490 (2003).

[16] A. Hohl, H.J.C. van der Linden, R. Roy, G. Goldsztein, F. Broner, and S.H. Strogatz, Phys. Rev. Lett. **74**, 2220 (1996).

[17] T.S. Dlodlo, Phys. Rev. **27**, 1435 (1983); IEEE J. Quantum Electron. **39**, 656 (2003).

[18] S.L. McCall, Appl. Phys. Lett. **32**, 284 (1978).

[19] T. Baer, J. Opt. Soc. Am. B **3**, 1175 (1986).

[20] R. Roy, T.W. Murphy, Jr., T.D. Maier, Z. Gills, and E.R. Hunt, Phys. Rev. Lett. **68**, 1259 (1992); K. Pyragas, F. Lange, T. Letz, J. Parisi, and A. Kittel, Phys. Rev. E **61**, 3721 (2000); A. Schenck zu Schweinsberg and U. Dressler, *ibid.* **63**, 056210 (2001).

[21] K. Pyragas, Phys. Lett. A **170**, 421 (1992).

[22] K. Ikeda and O. Akimoto, Opt. Commun. **30**, 257 (1979); K. Ikeda and K. Matsomoto, Physica D **29**, 223 (1987).

[23] H.M. Gibbs, F.A. Hopf, D.L. Kaplan, and R.L. Shoemaker, Phys. Rev. Lett. **46**, 474 (1981).

[24] T. Aida and P. Davis, IEEE J. Quantum Electron. **28**, 686 (1992).

[25] W.L. Chen, S.B. Wang, S.S. Twu, C.R. Chung, and Chin Pan, Int. J. Multiphase Flow **27**, 171 (2001); T.H.J.J. van der Hagen, D.D.B. van Bragt, F.J. van der Kaa, J. Karuza, D. Killian, W.H.M. Nissen, A.J.C. Stekelenburg, and J.A.A. Wouters, Ann. Nucl. Energy **24**, 659 (1997).

[26] J.K. Harbaugh and D. Stroud, Phys. Rev. B **56**, 8335 (1997).

[27] A.K. Jain, K.K. Likharev, J.E. Lukens, and J.E. Sauvageau, Phys. Rep. **109**, 309 (1984).

[28] A. Pikovsky, M. Rosenblum, and J. Kurths, *Synchronization: A universal Concept in Nonlinear Sciences* (Cambridge University Press, Cambridge, 2001).

[29] D.J. Christini and J.J. Collins, Phys. Rev. E **53**, R49 (1996).

[30] R.P. Klina and B.M. Baker, Int. J. Bifurcation Chaos Appl. Sci. Eng. **5**, 75 (1995).

[31] L.M. Pecora and T.L. Carroll, Phys. Rev. Lett. **67**, 945 (1991); T.L. Carroll and L.M. Pecora, Phys. Rev. E **48**, 2426 (1993).

[32] W. Yang, M. Ding, and H. Gang, Phys. Rev. Lett. **74**, 3955 (1995).

[33] L. Poon and C. Grebogi, Phys. Rev. Lett. **75**, 4023 (1995).

[34] Y.-C. Lai, Phys. Lett. A **221**, 375 (1996); Y. Jiang, *ibid.* **264**, 22 (1999); S. Kraut, U. Feudel, and C. Grebogi, Phys. Rev. E **59**, 5253 (1999).

[35] A.N. Pisarchik and B.K. Goswami, Phys. Rev. Lett. **84**, 1423 (2000).

[36] A.N. Pisarchik, Phys. Rev. E **64**, 046203 (2001).

[37] J.M. Saucedo-Solorio, A.N. Pisarchik, and V. Aboites, Phys. Lett. A **304**, 21 (2002).

[38] B.K. Goswami and S. Basu, Phys. Rev. E **66**, 026214 (2002).

[39] B. E. Martínez-Zérega, A. N. Pisarchik, and L. S. Tsimring, Phys. Lett. A **318**, 102 (2003).

[40] A. N. Pisarchik, Phys. Lett. A **318**, 65 (2003).

[41] *Rare Earth Doped Fiber Lasers and Amplifiers*, edited by M. Digonnet (Marcel Dekker, New York, 1993).

[42] M.W. Phillips, H. Gong, A.I. Ferguson, and D.C. Hanna, Opt. Commun. **61**, 215 (1987); G. Boulant, M. Lefranc, S. Bielawski, and D. Derozier, Phys. Rev. E **55**, 5082 (1997); D. Dangoisse, J.C. Celet, and P. Glorieux, *ibid.* **56**, 1396 (1997); T.C. Newell, A. Gavrielides, V. Kovanis, D. Sukow, T. Erneux, and S.A. Glasgow, *ibid.* **56**, 7223 (1997).

[43] F. Sanchez, P. LeBoudec, P.-L. François, and G. Stephan, Phys. Rev. A **48**, 2220 (1993); E. Lacot, F. Stoeckel, and M. Chenevier, *ibid.* **49**, 3997 (1993).

[44] L. Luo, T.J. Tee, and P.L. Chu, J. Opt. Soc. Am. B **15**, 972 (1998); Opt. Commun. **146**, 151 (1998); I.J. Sola, J.C. Martín, and J.M. Álvarez, *ibid.* **212**, 359 (2002); A.N. Pisarchik, Yu.O.

Barmenkov, and A.V. Kir'yanov, IEEE J. Quantum Electron. **39**, (2003).

[45] S. Colin, E. Contesse, P. Le Boudec, G. Stephan, and F. Sanchez, Opt. Lett. **21**, 1987 (1996).

[46] R. Rangel-Rojo and M. Mohebi, Opt. Commun. **137**, 98 (1997).

[47] M. Lakshmanan and K. Murali, in *Chaos in Nonlinear Oscillators*, edited by L. O. Chua (World Scientific, Singapore, 1996).

[48] P. Mandel and T. Erneux, Phys. Rev. Lett. **53**, 1818 (1984).

[49] A.N. Pisarchik, Phys. Lett. A **242**, 152 (1998); H.G. Davies and K. Rangavajhula, Proc. R. Soc. London, Ser. A **457**, 2965 (2001).

[50] A.N. Pisarchik and R. Corbalán, Physica D **150**, 14 (2001).